Towards a semiclassical justification of the 'effective random matrix theory' for transport through ballistic chaotic quantum dots

Piet W. Brouwer and Saar Rahav Laboratory of Atomic and Solid State Physics, Cornell University, Ithaca 14853, USA (Dated: September 25, 2018)

The scattering matrix S of a ballistic chaotic cavity is the direct sum of a 'classical' and a 'quantum' part, which describe the scattering of channels with typical dwell time smaller and larger than the Ehrenfest time, respectively. According to the 'effective random matrix theory' of Silvestrov, Goorden, and Beenakker [Phys. Rev. Lett. 90, 116801 (2003)], statistical averages involving the quantum-mechanical scattering matrix are given by random matrix theory. While this effective random matrix theory is known not to be applicable for quantum interference corrections to transport, which appear to subleading order in the number of scattering channels N, it is believed to correctly describe quantum transport to leading order in N. We here partially verify this belief, by comparing the predictions of the effective random matrix theory for the ensemble averages of polynomial functions of S and S^{\dagger} of degree 2, 4, and 6 to a semiclassical calculation.

PACS numbers: 73.23.-b,05.45.Mt,05.45.Pq,73.20.Fz

I. INTRODUCTION

For electrons moving in a ballistic conductor with chaotic classical dynamics there is a minimal time after which the wave nature of electrons becomes apparent: the Ehrenfest time. The Ehrenfest time $\tau_{\rm E}$ is the time it takes for classical trajectories initially a 'quantum distance' apart to separate and reach a 'classical distance'. Here, the quantum distance is the Fermi wavelength \hbar/p_F , where p_F is the Fermi momentum, whereas the classical distance can be taken to be the system size L or the width W of contacts connecting the sample to source and drain reservoirs. For chaotic classical dynamics with Lyapunov exponent λ , $\tau_{\rm E}$ is then determined by the condition $W=(\hbar/p_F)\exp(\lambda\tau_{\rm E})$, so that

$$\tau_{\rm E} = \frac{1}{\lambda} \ln \frac{p_F W}{\hbar}.\tag{1}$$

If the Ehrenfest time $\tau_{\rm E}$ is small in comparison to the mean dwell time $\tau_{\rm D}$ in the conductor and other time scales relevant for quantum transport (such as the dephasing time or the period of an applied AC bias) — which is true for most experimentally realized ballistic quantum dots⁴ —, the time threshold it poses for quantum processes is irrelevant, which explains why quantum signatures do not distinguish ballistic conductors from their disordered counterparts. Indeed, quantum transport in ballistic quantum dots with $\tau_{\rm E} \ll \tau_{\rm D}$ and quantum transport in disordered quantum dots are both described by random matrix theory.⁵

Recently, there has been considerable interest in the theoretical question what happens if the Ehrenfest time exceeds the mean dwell time $\tau_{\rm D}$. In this regime significant differences between the manifestations of quantum mechanics in ballistic chaotic and disordered conductors can occur. It is important to distinguish the effect of the Ehrenfest time on quantum phenomena that involve the splitting of trajectories only and quantum interfer-

ence phenomena, which involve the divergence of classical trajectories initially a quantum distance apart and their joining again. Examples of the former are shot noise^{6,7,8,9} and the excitation gap induced by the proximity to a superconductor. ^{10,11,12,13} Examples of the latter are weak localization, ^{1,14,15,16} universal conductance fluctuations, ^{17,18,19} and quantum corrections to the level density. ^{20,21} Here we focus on the first type of phenomena. The effects of the Ehrenfest time on quantum interference effects have proven quite subtle, and will not be discussed here (see the references cited above for details).

Silvestrov, Goorden, and Beenakker proposed a very attractive theoretical picture to describe Ehrenfest-time related phenomena in a ballistic chaotic quantum dot. 12 They noted that the dot's classical phase space can be divided into a part containing classical trajectories with dwell time shorter than $\tau_{\rm E}$ and a part with classical trajectories with dwell time longer than $\tau_{\rm E}$. Correspondingly, the dot's $N \times N$ scattering matrix $S(\varepsilon)$ is written as the direct sum of a scattering matrix $S_{\rm cl}(\varepsilon)$ for $N_{\rm c}$ 'classical channels' and a scattering matrix $S_{\rm q}(\varepsilon)$ for $N_{\rm q}$ 'quantum channels', with $N = N_{\rm c} + N_{\rm q}$,

$$S(\varepsilon) = \begin{pmatrix} S_{\rm cl}(\varepsilon) & 0\\ 0 & S_{\rm q}(\varepsilon) \end{pmatrix}. \tag{2}$$

The $N_{\rm c}$ -dimensional 'classical scattering matrix' $S_{\rm cl}(\varepsilon)$ represents fully deterministic scattering from the quantum dot, where all probability intensity is concentrated around one classical trajectory. The scattering phase shifts in $S_{\rm cl}(\varepsilon)$ follow from the dwell times of the corresponding classical trajectories. On the other hand, $S_{\rm q}(\varepsilon)$ represents quantum scattering, where the probability intensity is divided over a large number of scattering modes in all contacts. Writing

$$S_{\mathbf{q}}(\varepsilon) = e^{i\varepsilon\tau_{\mathbf{E}}}\tilde{S}_{\mathbf{q}}(\varepsilon),$$
 (3)

in order to factor out a trivial energy dependence arising from the fact that all trajectories contribution to $S_{\rm q}$ have

a minimal dwell time $\tau_{\rm E}$,^{13,22} Silvestrov, Goorden, and Beenakker proposed that the statistical distribution of $\tilde{S}_{\rm q}(\varepsilon)$ is that of random matrix theory,¹² provided $N_{\rm q}$ is large.

Since the original proposal of Ref. 12, it has been understood that this 'effective random matrix theory' does not provide a faithful description of all signatures of quantum transport. For example, the effective random matrix theory predicts that the weak localization correction to the conductance of a ballistic quantum dot is Ehrenfest-time independent, whereas both microscopic semiclassical theory and numerical simulations find an exponential dependence on $\tau_{\rm E}/\tau_{\rm D}$. 1,14,15,16,19 Weak localization is a quantum interference effect, which arises as a correction to subleading order in the total channel number N. The effective random matrix theory has been successful in predicting and explaining Ehrenfest-time dependences that appear to leading order in N, such as shot noise, ^{6,7,8,9} the proximity-induced gap in a quantum dot coupled to a superconductor, ^{10,11,12,13,23} the density of transmission eigenvalues, ²⁴ and the probability distribution of lifetimes of quasibound states in chaotic quantum $\rm dots.^{25}$

Whereas the effective random matrix theory has been compared to the results of accurate numerical simulations in all four examples mentioned above, the microscopic verification of the effective random matrix theory is limited to a theoretical construction of the decomposition $(2)^{18}$ and to the comparison of the effective random matrix theory and microscopic calculations of the $\tau_{\rm E}$ dependence of the shot noise power of a chaotic quantum dot^{6,9} and the density of states of a quantum dot coupled to a superconductor (an 'Andreev quantum dot') for energies much larger than the proximity-induced energy gap. 11 (For energies comparable to the energy gap, the theory of Ref. 11 makes use of an ansatz that is similar in spirit to the ansatz of effective random matrix theory.) The comparison to a microscopic calculation of shot noise amounts to a test of the effective random matrix theory for traces of polynomial functions of the scattering matrix S and its hermitian conjugate S^{\dagger} of degree 4. The comparison to the density of states of an Andreev quantum dot at high energies addresses of the statistics of polynomials of $S_{\rm cl}(\varepsilon)S_{\rm cl}^*(-\varepsilon)$ of arbitrary degree, but not of S_{q} . The aim of this article is to provide the next step towards a microscopic verification of the effective random matrix theory by comparing a semiclassical theory of the ensemble average of a trace of a degree-six polynomial function of S and S^{\dagger} with the predictions of the effective random matrix theory. Since the hypothesis of the effective random matrix was formulated after the microscopic calculations of the Ehrenfest-time dependence of shot noise and the density of states in an Andreev quantum dot, we believe that this calculation is the first nontrivial test of the effective random matrix theory.

In Sec. II below we review the predictions of the effective random matrix theory for the averages of traces of polynomials of S and S^{\dagger} of degree two, four, and six. We follow with a semiclassical calculation of these averages in Sec. III and conclude in Sec. IV. Details of the calculations can be found in the two appendices.

II. PREDICTIONS OF THE EFFECTIVE RANDOM MATRIX THEORY

In our calculation, we consider a ballistic quantum dot coupled to electron reservoirs through ballistic point contacts. Hence, the scattering matrix S acquires a block structure $S = S_{ij}$, where the indices i and j label the point contacts. The dimension of the block S_{ij} is $N_i \times N_j$, where N_i is the number of channels in the ith point contact. Each block S_{ij} can be decomposed into a 'classical' and a 'quantum' scattering matrix as in Eq. (2).

We are interested in averages of the form

$$\begin{split} Q_2 &= \frac{1}{N} \langle \operatorname{tr} S_{ij}(\varepsilon_1) S_{ij}^{\dagger}(\varepsilon_2) \rangle, \\ Q_4 &= \frac{1}{N} \langle \operatorname{tr} S_{ij}(\varepsilon_1) S_{kj}^{\dagger}(\varepsilon_2) S_{kl}(\varepsilon_3) S_{il}^{\dagger}(\varepsilon_4) \rangle, \\ Q_6 &= \frac{1}{N} \langle \operatorname{tr} S_{ij}(\varepsilon_1) S_{kj}^{\dagger}(\varepsilon_2) S_{kl}(\varepsilon_3) \dots S_{in}^{\dagger}(\varepsilon_6) \rangle. \end{split} \tag{4}$$

The polynomials Q_2 and Q_4 describe, e.g., the conductance and shot noise power of a quantum dot with normal-metal contacts, whereas polynomials of higher degree are necessary for a theory of transport and equilibrium properties of quantum dots with superconducting contacts. According to the effective random matrix theory, these averages have the structure

$$Q_n = \left[1 - e^{-F_n(1,\dots,n)\tau_{\rm E}/\tau_{\rm D}}\right] Q_n^{\rm cl} + e^{-F_n(1,\dots,n)\tau_{\rm E}/\tau_{\rm D}} Q_n^{\rm RMT},$$
 (5)

where the function F_n is defined as

$$F_n(1,...,n) = 1 + \frac{i\tau_D}{\hbar} \sum_{j=1}^n (-1)^j \varepsilon_j,$$
 (6)

and $Q^{\rm cl}$ and $Q^{\rm RMT}$ are obtained from Eq. (4) by replacing S by $S_{\rm cl}$ and $\tilde{S}_{\rm q}$ and N by $N_{\rm c}$ and $N_{\rm q}$, respectively. The classical averages $Q_{\rm cl}^{\rm cl}$ read¹²

$$Q_n^{\text{cl}} = \frac{N_i N_j}{N^2 F_2(1, 2)}.$$

$$Q_4^{\text{cl}} = \frac{N_i N_j \delta_{ik} \delta_{jl}}{N^2 F_4(1, 2, 3, 4)},$$

$$Q_6^{\text{cl}} = \frac{N_i N_j \delta_{ik} \delta_{jl} \delta_{im} \delta_{jn}}{N^2 F_6(1, 2, 3, 4, 5, 6)}.$$
(7)

The random matrix average of the trace of a degree two polynomial of S and S^{\dagger} is equal to the classical average, ²⁷

$$Q_2^{\rm RMT} = Q_2^{\rm cl}. \tag{8}$$

However, the higher-order random matrix averages are different. For Q_4 one has²⁸

$$Q_4^{\text{RMT}} = \frac{N_i N_j N_l \delta_{ik}}{N^3 F_2(1, 2) F_2(3, 4)} + \frac{N_i N_j N_k \delta_{jl}}{N^3 F_2(3, 2) F_2(1, 4)} - \frac{N_i N_j N_k N_l F_4(1, 2, 3, 4)}{N^4 F_2(1, 2) F_2(3, 2) F_2(3, 4) F_2(1, 4)}, \tag{9}$$

whereas the random matrix average Q_6 reads²⁹

$$Q_{6}^{\text{RMT}} = \frac{N_{i}N_{j}N_{l}N_{n}\delta_{ik}\delta_{im}}{N^{4}F_{2}(1,2)F_{2}(3,4)F_{2}(5,6)} + \frac{N_{i}N_{j}N_{k}N_{m}\delta_{jl}\delta_{jn}}{N^{4}F_{2}(3,2)F_{2}(5,4)F_{2}(1,6)} - \frac{N_{i}N_{j}N_{k}N_{l}N_{m}N_{n}F_{6}(1,2,3,4,5,6)}{F_{2}(1,2)F_{2}(3,2)F_{2}(3,4)F_{2}(5,4)F_{2}(5,6)F_{2}(1,6)} + \left[\frac{N_{i}N_{j}N_{l}N_{m}\delta_{ik}\delta_{ln}}{N^{4}F_{2}(1,2)F_{2}(3,6)F_{2}(5,4)} + \frac{N_{i}N_{j}N_{k}N_{l}N_{m}N_{n}F_{4}(1,2,3,4)F_{4}(1,4,5,6)}{F_{2}(1,2)F_{2}(3,2)F_{2}(3,4)F_{2}(5,4)F_{2}(5,6)F_{2}(1,6)} - \frac{N_{i}N_{j}N_{k}N_{m}N_{n}F_{4}(1,4,5,6)\delta_{jl}}{N^{5}F_{2}(1,2)F_{2}(3,4)F_{2}(5,4)F_{2}(5,6)F_{2}(3,6)} - \frac{N_{i}N_{j}N_{k}N_{m}N_{n}F_{4}(1,4,5,6)\delta_{jl}}{N^{5}F_{2}(1,2)F_{2}(3,4)F_{2}(5,4)F_{2}(5,6)F_{2}(3,6)} + \dots \right], (10)$$

where the dots ... refer to the simultaneous cyclic permutations $(1, 2, i, j) \rightarrow (3, 4, k, l) \rightarrow (5, 6, m, n)$.

Together, Eqs. (5), (7), (8), (9), and (10) specify the prediction of the effective random matrix theory for the averages of the traces of polynomials of the scattering matrix and its hermitian conjugate for polynomials up to degree 6.

III. SEMICLASSICAL CALCULATION

We now perform a semiclassical calculation of the averages Q_2 , Q_4 , and Q_6 defined in Eq. (4) above and show that they agree with the predictions of the effective random matrix theory as described in the previous section. Although semiclassical calculations of Q_2 and Q_4 exist, see Refs. 27,30,31,32 and 6,9,33, respectively, we briefly review their derivation in order to establish the context for the calculation of Q_6 . (We are not aware of a semiclassical calculation of the energy dependence of Q_4 , however.)

In our calculation, we take the limit $\hbar \to 0$ while keeping the ratios $\tau_{\rm E}/\tau_{\rm D}$ and N_i/N , and the products $\tau_{\rm D}\varepsilon_i/\hbar$ fixed. The latter condition implies that the functions F_n defined in Eq. (6) remain constant in the limiting procedure. Note that the channel numbers N_i diverge in this limit. The divergence of the channel numbers does not affect Q_2 , Q_4 , or Q_6 , however, because these depend on the ratios N_i/N only. Since $\tau_{\rm E} \propto \ln(1/\hbar)$, see Eq. (1), the condition that the ratio $\tau_{\rm E}/\tau_{\rm D}$ is kept constant in the limiting procedure implies that the dwell time $\tau_{\rm D}$ diverges as well. The divergence of $\tau_{\rm D}$ removes any dependence on the non-universal short-time dynamics in the quantum dot.

Starting point of our calculation is an expression of the dot's scattering matrix S as a sum over classical trajectories $\alpha, ^{30,31,32}$

$$(S_{ij})_{mn} = \left(\frac{\pi\hbar}{2W_iW_j}\right)^{1/2} \sum_{\alpha} A_{\alpha} e^{i\mathcal{S}_{\alpha}/\hbar}, \qquad (11)$$

where i and j label the exit and entrance leads, respec-

tively, and m and n label the propagating modes in these leads. The widths of the entrance and exit contacts are W_j and W_i , respectively. The trajectory α connects the entrance contact j to the exit contact i. The components p_{\perp} and p'_{\perp} of its momentum perpendicular to the lead axis upon entrance and exit, respectively, are compatible with that of the modes n and m in the corresponding leads,

$$p_{\perp} = \pm \pi \hbar n / W_j, \quad n = 1, \dots, N_j,$$

 $p'_{\perp} = \pm \pi \hbar m / W_i, \quad m = 1, \dots, N_i.$ (12)

(Here and in the remainder of this article, primed variables refer to the exit contact.) Further, S_{α} is the classical action of trajectory α and A_{α} is its stability amplitude. The latter is defined as

$$A_{\alpha} = \left| \frac{\partial p_{\perp}'}{dy} \right|^{-1/2},\tag{13}$$

where y is the coordinate perpendicular to the axis of the entrance contact, see Fig. 1, and the partial derivative is taken at constant p_{\perp} . The classical action \mathcal{S}_{α} is a function of p_{\perp} and p'_{\perp} . The spatial coordinates y and y' of the trajectory α upon entrance and exit can be expressed as derivatives of \mathcal{S}_{α} ,

$$y = \frac{\partial S_{\alpha}}{\partial p_{\perp}}, \quad y' = -\frac{\partial S_{\alpha}}{\partial p'_{\perp}}.$$
 (14)

For simplicity of notation, the Maslov index and other phase shifts are included in S_{α} .

We are interested in the scattering matrix S_{ij} at different values of the energy ε . The energy ε enters in Eq. (11) through the energy dependence of the action S_{α} ,

$$S_{\alpha}(\varepsilon) = S_{\alpha}(\varepsilon_0) + (\varepsilon - \varepsilon_0)t_{\alpha}, \tag{15}$$

where ε_0 is a reference energy and t_{α} is the duration of the trajectory α . We neglect the energy dependence of the stability amplitudes A_{α} .

Using Eq. (11), the traces Q_n , n = 2, 4, 6, are expressed as double, quadruple, and sixfold summations over clas-

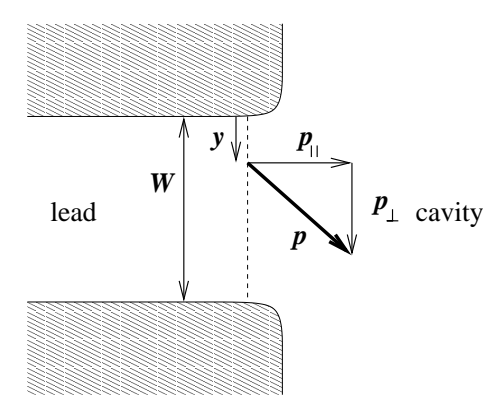


FIG. 1: Schematic drawing of one of the contacts to the quantum dot. The coordinate y as well as the perpendicular component of the momentum p_{\perp} refers to the direction perpendicular to the lead axis. In the sum (11) over classical trajectories there is no restriction on y, but only discrete values of p_{\perp} are considered.

sical trajectories,

$$Q_2 = \frac{\pi\hbar}{2W_i W_j} \sum_{\alpha_1, \alpha_2} A_1 A_2 e^{i(\mathcal{S}_1 - \mathcal{S}_2)/\hbar}, \qquad (16)$$

with similar expressions for Q_4 and Q_6 . Here and in the remainder of this article we use the indices 1 and 2 to denote α_1 and α_2 if possible without confusion. The transverse momentum components p_{\perp} and p'_{\perp} at the entrance and exit contacts of the n trajectories involved in the trajectory sum for Q_n satisfy

$$p_{\perp,1} = p_{\perp,2}, \dots, p_{\perp,n-1} = p_{\perp,n},$$

 $p'_{\perp,2} = p'_{\perp,3}, \dots, p'_{\perp,n} = p'_{\perp,1},$ (17)

where $n=2,4,6.^{40}$ In the summation (16), the magnitudes of all transverse momentum components are taken equal to the quantized values (12). However, for large channel numbers we may replace the summation over the quantized momenta by integrations over p_{\perp} and $p_{\perp'}$, so that

$$Q_2 = \frac{1}{2\pi\hbar} \int dp_{\perp,1} dp'_{\perp,1} \sum_{\alpha_1,\alpha_2} A_1 A_2 e^{i(S_1 - S_2)/\hbar}, (18)$$

again with similar expressions for Q_4 and Q_6 . In Eq. (18) and its equivalents for Q_4 and Q_6 , one integrates over the perpendicular momentum components p_{\perp} and p'_{\perp} of the trajectories $\alpha_1, \ldots, \alpha_{n-1}$ with odd indices. The initial and final transverse momentum components of the classical trajectories $\alpha_2, \ldots, \alpha_n$ with even indices are determined by the conditions (17).

For the calculations below, we assume that the classical dynamics inside the quantum dot is uniformly hyperbolic. This assumption simplifies the calculations, although it is believed not to affect the final results in the universal limit $\tau_{\rm D} \gg L/v_F$. ^{34,35,36} With uniformly hyperbolic classical dynamics, the optimal phase space

coordinates for a Poincaré surface of section taken in the interior of the quantum dot are coordinates s and u taken along the stable and unstable directions in phase space. In view of this, we replace the trajectory sum (18), which is taken over trajectories with specified transverse momentum components p_{\perp} and p'_{\perp} at entrance and exit contacts, by a trajectory sum over trajectories with specified stable and unstable phase space coordinates s and u' at entrance and exit contacts, respectively. Referring to App. A for details, we find that the traces Q_2 , Q_4 , and Q_6 can also be expressed as

$$Q_{2} = \frac{1}{2\pi\hbar} \int ds_{1} du'_{1} \sum_{\alpha_{1},\alpha_{2}} A_{1} A_{2} e^{i(S_{1} - S_{2})/\hbar}, \quad (19)$$

$$Q_{4} = \frac{1}{(2\pi\hbar)^{2}} \int ds_{1} du'_{1} ds_{3} du'_{3}$$

$$\times \sum_{\alpha_{1},\dots,\alpha_{4}} A_{1} \dots A_{4} e^{i(S_{1} - \dots - S_{4})/\hbar}, \quad (20)$$

$$Q_{6} = \frac{1}{(2\pi\hbar)^{3}} \int ds_{1} du'_{1} ds_{3} du'_{3} ds_{5} du'_{5}$$

$$\times \sum_{\alpha_{1},\dots,\alpha_{6}} A_{1} \dots A_{6} e^{i(S_{1} - \dots - S_{6})/\hbar}, \quad (21)$$

where the classical trajectories α_{μ} , $\mu = 1, ..., n$ satisfy the conditions

$$s_1 = s_2, \dots, s_{n-1} = s_n,$$

 $u'_2 = u'_3, \dots, u'_n = u'_1,$ (22)

with n=2,4,6. Further, in Eqs. (19)–(21), the stability amplitudes are defined as

$$A_{\alpha} = \left| \frac{\partial u'}{\partial u} \right|^{-1/2},\tag{23}$$

and the classical actions $S_{\alpha}(s, u')$ are Legendre transforms of the original classical actions $S_{\alpha}(p_{\perp}, p'_{\perp})$, so that

$$\frac{\partial S_{\alpha}}{\partial s} = u_{\alpha}, \quad \frac{\partial S_{\alpha}}{\partial u'} = -s'_{\alpha}. \tag{24}$$

For the interpretation of Eqs. (19)–(21), one should keep in mind that the phase space coordinates s and u are defined only locally. That means that the coordinate transformation $(x, p_{\perp}) \to (s, u)$ can only be made for pairs of trajectories that enter or exit the quantum dot at nearby phase space points. This poses no problems for our calculation, because only classical trajectories that exit the quantum dot at nearby positions and with close momenta have an action difference $\Delta \mathcal{S}$ that varies sufficiently slowly as a function of the phase space coordinates to give a finite contribution to Q_n , n=2,4,6. Indeed, the explicit calculations of Q_2 , Q_4 , and Q_6 in the following subsections show that the entire contribution to Q_n comes from trajectories for which the differences of the stable or unstable phase space coordinates are small.

A. Calculation of Q_2

The leading contribution to Q_2 arises from equal trajectories $\alpha_1 = \alpha_2$. In that case, the action difference

$$\Delta S = S_1 - S_2$$

= $(\varepsilon_1 - \varepsilon_2)t$, (25)

where t is the common duration of the trajectories α_1 and α_2 . The stability amplitudes are equal, $A_1 = A_2 = A$. The factor $A_1A_2 = A^2$ in Eq. (19) provides the Jacobian necessary to replace the integration over the unstable phase space coordinate u' at the exit contact by an integration over the unstable phase space coordinate u at the entrance contact. 30,31,32 This way, Q_2 is expressed in terms of an integration over the phase space coordinates s and u at a Poincaré surface of section taken in the entrance contact. Equivalently, the double integral over s and u' can be represented by a phase space integral over any Poincaré surface of section taken anywhere along the classical trajectory $\alpha_1 = \alpha_2$. Following the latter strategy, we write Q_2 as

$$Q_{2} = \int dq \int_{0}^{\infty} dt_{1} dt_{2} \frac{P_{i}(t_{1})P_{j}(t_{2})e^{i(\varepsilon_{1}-\varepsilon_{2})(t_{1}+t_{2})/\hbar}}{2\pi\hbar(t_{1}+t_{2})N},$$
(26)

where q refers to the phase space coordinate at which the reference surface of section is taken, $P_i(t_1)$ selects only those q for which the classical propagation of q ends up in contact i after time t_1 , and $P_j(t_2)$ selects q for which the classical propagation of the time-reversed of q ends at contact j after a time t_2 . We divided by $t = t_1 + t_2$ to cancel a spurious contribution from the freedom to choose the reference surface of section at an arbitrary point along the trajectory $\alpha_1 = \alpha_2$. Replacing P_i and P_j by classical probabilities to reach the contacts i and j for an arbitrary phase space point q,

$$P_i(t) = \frac{N_i}{N\tau_{\rm D}} e^{-t/\tau_{\rm D}}, \quad P_j(t) = \frac{N_j}{N\tau_{\rm D}} e^{-t/\tau_{\rm D}},$$
 (27)

the integration over q contributes the total phase space volume $2\pi\hbar N\tau_{\rm D}$ of the quantum dot and we find the well-known result

$$Q_2 = \frac{N_i N_j}{N^2 F_2(1, 2)} \tag{28}$$

upon integration over t_1 and t_2 .

B. Calculation of Q_4

The trace Q_4 is expressed as a quadruple sum over classical trajectories, see Eq. (20). The typical configuration of four trajectories that contributes to Q_4 was pointed out in Refs. 9,33: The trajectories α_1 , α_2 , α_3 , and α_4 , which are paired close to entrance and exit, have a small-angle encounter at which the pairing of the trajectories is interchanged, see Fig. 2. Before arriving at

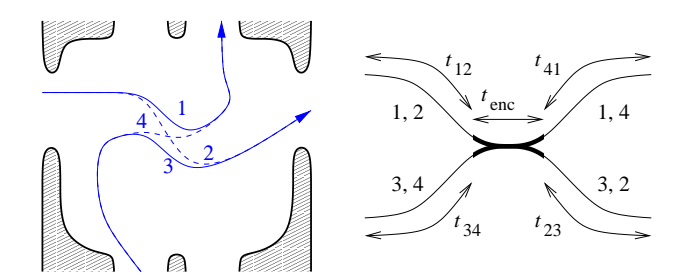


FIG. 2: Left: Four classical trajectories that give the random matrix contribution to the average Q_4 . These trajectories have a small-angle encounter which fully resides inside the quantum dot. Right: Schematic drawing of the encounter together with the definitions of the various times used in the text. The encounter region is shown thick.

the encounter, α_1 and α_2 , and α_3 and α_4 are paired. After the encounter, α_2 and α_3 , and α_4 and α_1 are paired. The encounter may reside fully inside the quantum dot, as in Fig. 2, so that the pairs of trajectories are uncorrelated when they exit and enter the quantum dot, or the small-angle encounter may touch one or two of the lead openings, as in Figs. 3 and 4, respectively, so that exit or entrance of the four trajectories is correlated. While the importance of such small-angle encounters of classical trajectories was first realized for weak localization, ^{1,37} they play a crucial role in all semiclassical theories of quantum transport. ^{9,14,16,19,33,34}

Since all four trajectories are fixed once we have specified α_1 and α_3 , we need to sum over α_1 and α_3 only. In order to parameterize α_1 and α_3 we take a Poincaré surface of section chosen at an arbitrary point during the encounter. We then use the coordinate q of a reference point at the Poincaré surface of section, as well as the differences $s_3 - s_1$ and $u_3 - u_1$ of the stable and unstable phase space coordinates to parameterize α_1 and α_3 . The trajectories α_1 and α_2 , and α_3 and α_4 originate from the same contact and with the same stable phase stable space coordinate, hence

$$s_1 = s_2, \quad s_3 = s_4.$$
 (29)

Similarly,

$$u_4 = u_1, \quad u_2 = u_3. \tag{30}$$

Since the trajectory pairs have the same stable and unstable phase space coordinates at the entrance and exit contacts, respectively, the conditions (29) and (30) hold for encounters that do not touch the contacts as well as for encounters that touch the contacts.

We first discuss the case of Fig. 2, in which the encounter resides fully inside the quantum dot. We closely follow Ref. 33, in which the same configuration of trajectories was considered in the limit $\tau_{\rm E}/\tau_{\rm D} \to 0$. The encounter region is defined as the segment of the trajectories for which $|s_1 - s_3| < c$ and $|u_1 - u_3| < c$, where $c \sim (p_F W)^{1/2}$ is a classical cut-off below which the classical dynamics can be linearized. The precise choice of

W is irrelevant in the classical limit, see the discussion following Eq. (37). Hence, the duration of the encounter is

$$t_{\rm enc} = \frac{1}{\lambda} \ln \frac{c^2}{|(u_3 - u_1)(s_3 - s_1)|},\tag{31}$$

where λ is the Lyapunov exponent for the classical dynamics in the quantum dot. We parameterize the durations t_{α_1} , t_{α_2} , t_{α_3} , and t_{α_4} of the four trajectories involved using $t_{\rm enc}$ and the durations t_{12} , t_{23} , t_{34} , and t_{41} of the four stretches connecting the encounter region with the lead openings,

$$t_{\alpha_{1}} = t_{\text{enc}} + t_{12} + t_{41},$$

$$t_{\alpha_{2}} = t_{\text{enc}} + t_{12} + t_{23},$$

$$t_{\alpha_{3}} = t_{\text{enc}} + t_{34} + t_{23},$$

$$t_{\alpha_{4}} = t_{\text{enc}} + t_{34} + t_{41}.$$
(32)

Schematically, the definitions of $t_{\rm enc}$ and of the times t_{12} , t_{23} , t_{34} , and t_{41} are shown in the right panel of Fig. 2. The action difference ΔS is the symplectic area enclosed by the four trajectories, ^{38,39} plus a contribution from the energy differences,

$$\Delta S = (s_3 - s_1)(u_3 - u_1) + t_{\text{enc}}(\varepsilon_1 - \varepsilon_2 + \varepsilon_3 - \varepsilon_4) + t_{12}(\varepsilon_1 - \varepsilon_2) + t_{23}(\varepsilon_3 - \varepsilon_2) + t_{34}(\varepsilon_3 - \varepsilon_4) + t_{41}(\varepsilon_1 - \varepsilon_4).$$
(33)

Note that the enclosed phase space areas are conserved along the motion of the trajectories. In particular, this means that the action difference ΔS is independent of where the Poincaré surface of section is chosen.

Integrating over the position of the Poincaré surface of section, we then find

$$Q_4^{(2)} = \int dt_{12} dt_{23} dt_{34} t_{41} P_j(t_{12}) P_k(t_{23}) P_l(t_{34}) P_i(t_{41})$$

$$\times \int d(u_3 - u_1) d(s_3 - s_1) \frac{\tau_D e^{i\Delta S/\hbar - t_{\text{enc}}/\tau_D}}{2\pi \hbar t_{\text{enc}}}.$$
(34)

In this equation, the factor $t_{\rm enc}$ in the denominator cancels a spurious contribution to the integral from the freedom to choose the Poincaré surface of section anywhere along the encounter region. The classical probabilities $P_i(t_{41})$, $P_j(t_{12})$, $P_k(t_{23})$, and $P_l(t_{34})$ are defined as in Eq. (27). The factor $\exp(-t_{\rm enc}/\tau_{\rm D})$ is the probability that the trajectories do not exit the quantum dot during the encounter stretch. (If they do, the encounter touches the lead opening. This case is treated separately below.)

Taking $u_3 - u_1$ to be positive (while adding a factor 2 in Eq. (34)), we perform the variable change

$$u_3 - u_1 = c/\sigma, \quad s_3 - s_1 = cx\sigma.$$
 (35)

With the new integration variables, the integration domain is -1 < x < 1 and $1 < \sigma < 1/|x|$. Further,

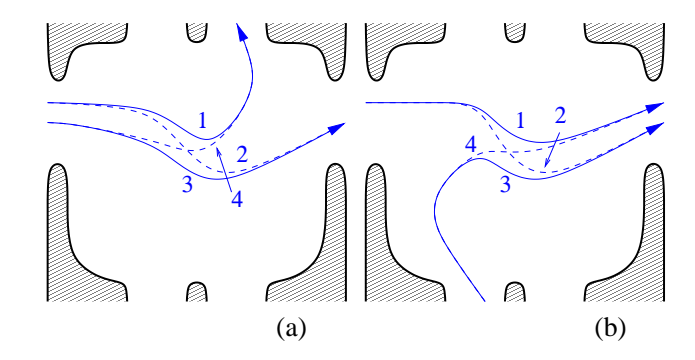


FIG. 3: Schematic drawing of four classical trajectories that give the random matrix contribution with one Kronecker delta to the average Q_4 . These trajectories have a small-angle encounter touches one of the lead openings. The Kronecker delta appears for the entrance lead index in (a) and for the exit lead index in (b).

 $t_{\rm enc} = \lambda^{-1} \ln(1/|x|)$. Integrating over t_{12} , t_{23} , t_{34} , and t_{41} , and σ , and performing a partial integration to x, we then find

$$Q_4^{(2)} = -\frac{N_i N_j N_k N_l F_4(1, 2, 3, 4)}{N^4 F_2(1, 2) F_2(3, 2) F_2(3, 4) F_2(1, 4)} \times \int_0^1 dx x^{F_4(1, 2, 3, 4)/\lambda \tau_D} \frac{2 \sin(xr)}{\pi x}, \quad (36)$$

where we omitted a term that is an oscillating function of $r=c^2/\hbar$ in the limit $\hbar \to 0$. The remaining integral over x can be evaluated in the limit $\hbar \to 0$ at fixed $\tau_{\rm E}/\tau_{\rm D}$, and we arrive at the final result

$$Q_4^{(2)} = -\frac{N_i N_j N_k N_l F_4(1, 2, 3, 4)}{N^4 F_2(1, 2) F_2(3, 2) F_2(3, 4) F_2(1, 4)} \times e^{-\tau_{\rm E} F_4(1, 2, 3, 4) / \tau_{\rm D}},$$
(37)

where the Ehrenfest time $\tau_{\rm E}$ is defined as, cf. Eq. (1),

$$\tau_{\rm E} = \frac{1}{\lambda} \ln r = \frac{1}{\lambda} \ln \frac{c^2}{\hbar}.$$
 (38)

It is important to notice that the precise value of the phase-space cut-off c enters only through the Ehrenfest time $\tau_{\rm E}$. However, since the Ehrenfest time appears in the combination $\tau_{\rm E}/\tau_{\rm D}$ only and since $\tau_{\rm D} \to \infty$ in the classical limit taken here, any change of c by a factor of order unity will not affect the final result. It is because of this that we did not need to carefully specify the classical length scale W entering into the cut-off c.

If the encounter region touches one of the lead openings, as in Figs. 3a and b, a slight modification of the above calculation is called for. For definiteness, we consider an encounter that touches the entrance lead opening, as shown in Fig. 3a. This implies j=l, so that the corresponding contribution to Q_4 is proportional to δ_{jl} . The action difference ΔS is given by Eq. (33) with $t_{12}=t_{34}=0$. Since the trajectories α_1 and α_3 must be

correlated upon entry for the configuration shown in Fig. 3a, the encounter time $t_{\rm enc}$ is bounded by

$$0 < t_{\rm enc} - \frac{1}{\lambda} \ln \frac{c}{|u_3 - u_1|} < \frac{1}{\lambda} \ln \frac{c}{|s_3 - s_1|}.$$
 (39)

Then, proceeding as in the calculation of $Q_4^{(2)}$ and integrating over t_{23} and t_{41} , we find

$$Q_4^{(3a)} = \frac{N_i N_k \tau_{\rm D} \delta_{jl}}{N^2 F_2(3, 2) F_2(1, 4)} \int dt_{\rm enc} P_j(t_{\rm enc}) \times \int_{-c}^{c} \frac{d(s_1 - s_3) d(u_1 - u_3)}{2\pi \hbar t_{\rm enc}} \times e^{i(s_3 - s_1)(u_3 - u_1)/\hbar + it_{\rm enc}(\varepsilon_1 - \varepsilon_2 + \varepsilon_3 - \varepsilon_4))/\hbar}. (40)$$

In order to perform the integrations in Eq. (40), we take $u_3 - u_1$ to be positive and perform the variable change

$$u_3 - u_1 = \frac{c}{\sigma}, \quad s_3 - s_1 = cx\sigma.$$
 (41)

With the new integration variables, the integration domain is -1 < x < 1, $1 < \sigma < e^{\lambda t_{\rm enc}}$, and $0 < t_{\rm enc} < \lambda^{-1} \ln(1/|x|)$. Hence, with $r = c^2/\hbar$ and integrating over $t_{\rm enc}$ and σ , the integral (40) becomes

$$Q_4^{(3a)} = \frac{N_i N_j N_k \delta_{jl}}{N^3 F_2(3, 2) F_2(1, 4)} \times \int_0^1 dx \frac{2 \sin(rx)}{\pi x} x^{F_4(1, 2, 3, 4)/\lambda \tau_D} = \frac{N_i N_j N_k \delta_{jl}}{N^3 F_2(3, 2) F_2(1, 4)} e^{-\tau_E F_4(1, 2, 3, 4)/\tau_D}, (42)$$

where, again, we omitted terms proportional to $\sin r$. Similarly, for $Q_4^{(3b)}$ one finds

$$Q_4^{(3b)} = \frac{N_i N_j N_l \delta_{ik}}{N^3 F_2(3,4) F_2(1,2)} e^{-\tau_{\rm E} F_4(1,2,3,4)/\tau_{\rm D}}. (43)$$

Finally, if the encounter touches both lead openings, one has

$$Q_{4}^{(4)} = \tau_{D} \int dt_{1} dt_{2} \frac{P_{i}(t_{1})P_{j}(t_{2})}{t_{enc}} \delta_{ik} \delta_{jl}$$

$$\times \int d(s_{3} - s_{1}) d(u_{3} - u_{1}) \frac{e^{i\Delta S/\hbar}}{2\pi\hbar}, \quad (44)$$

where P_i and P_j are classical probabilities given in Eq. (27), t_1 and t_2 are the propagation times between the surface of section and the exit contact and the entrance contact and the surface of section, respectively, and $t_{\rm enc} = t_1 + t_2$. The action difference $\Delta \mathcal{S}$ is given by Eq. (33) with $t_{12} = t_{23} = t_{34} = t_{41} = 0$. In order to ensure that α_1 and α_3 are correlated upon entrance as well as exit, we require

$$t_1 < \frac{1}{\lambda} \ln \frac{c}{|s_3 - s_1|}, \quad t_2 < \frac{1}{\lambda} \ln \frac{c}{|u_3 - u_1|}.$$
 (45)

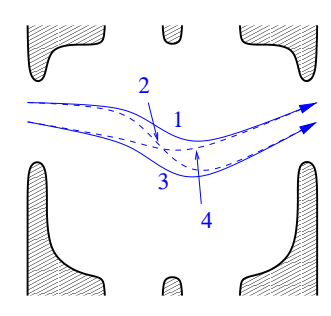


FIG. 4: Schematic drawing of four classical trajectories with a small-angle encounter that touches both lead openings. Such configurations of classical trajectories give the classical contribution to Q_4 .

Performing integrations to $t_1 - t_2$ and $u_3 - u_1$ and abbreviating $x = (s_3 - s_1)c$, one finds

$$Q_4^{(4)} = \delta_{ik}\delta_{jl}\frac{N_iN_j}{N^2}\int \frac{dt}{\tau_D}e^{-t/\tau_D+it(\varepsilon_1-\varepsilon_2+\varepsilon_3-\varepsilon_4)} \times \int_0^{e^{-\lambda t}} \frac{dx}{x}\frac{2\sin(xr)}{\pi}.$$
 (46)

The integral over x has to be performed in the limit $r \to \infty$ at fixed ratio τ_E/t . Since

$$\int_0^{e^{-\lambda t}} \frac{dx}{x} \frac{2\sin(xr)}{\pi} = \theta(\tau_E - t)$$
 (47)

if $r \to \infty$, where $\theta(x) = 1$ if x > 0 and 0 otherwise, we find

$$Q_4^{(4)} = \frac{N_i N_j \delta_{ik} \delta_{jl}}{N^2 F_4(1, 2, 3, 4)} (1 - e^{-\tau_{\rm E} F_4(1, 2, 3, 4)/\tau_{\rm D}}). (48)$$

Together, Eqs. (37), (42), (43), and (48) reproduce the prediction of the effective random matrix theory.

We note that there is a close connection between the appearance of Kronecker deltas involving the contact indices i, j, k, and l, and the configurations of classical trajectories that contribute to Q_4 : each encounter region that touches a lead opening gives rise to a Kronecker delta and, conversely, each Kronecker delta derived from an encounter that touched a lead opening. Hence, the four contributions to Q_4 — the third line in Eq. (7) and the three terms in Eq. (9) —, each of which have a different product of Kronecker deltas, are in a one-to-one correspondence with the four configurations of classical trajectories shown in Figs. 2, 3a, 3b, and 4,

We should point out that, without dependence on the energy arguments, *i.e.*, after setting $\varepsilon_1 = \varepsilon_2 = \varepsilon_3 = \varepsilon_4$, the semiclassical calculation of Q_4 was first performed by Whitney and Jacquod.⁹ The same results can also be inferred from an earlier calculation by Agam, Aleiner, and Larkin, who used a different formalism.⁶ The energy dependence of the four terms we calculate here is nontrivial, however, and clearly reveals the structure of the classical trajectories underlying the four different terms in the average.

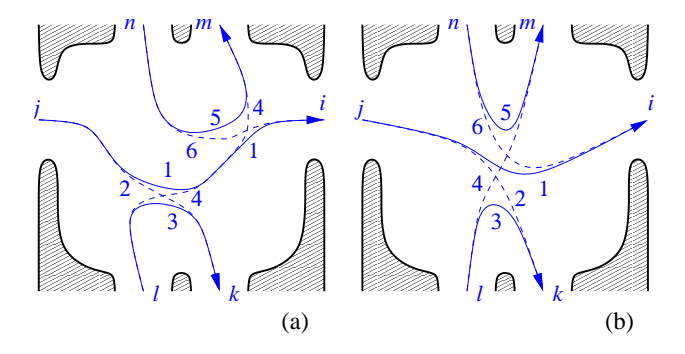


FIG. 5: Schematic drawing of six classical trajectories that contribute to Q_6 without encounters that touch the lead openings. The configuration shown in (a) consists of two separate two-encounters. There are two more configurations of this type, which are obtained by the cyclic permutations $(1,2) \rightarrow (3,4) \rightarrow (5,6)$. The configuration shown in (b) consists of one three-encounter.

While our calculation of $Q_4^{(2)}$ closely followed that of Braun *et al.*, ³³ our calculation of the remaining three contributions to Q_4 differs considerably from that of Ref. 33. Braun et al. do not consider encounters that touch the lead openings. Instead, they calculate the remaining contributions to Q_4 using the 'diagonal approximation' for the trajectory sums. Although this approximation gives the correct result if $\tau_{\rm E} \ll \tau_{\rm D}$, it is based on a different class of trajectories than the ones we considered (see also Ref. 9). In the diagonal approximation, one considers the case that the four trajectories α_1 , α_2 , α_3 , and α_4 are pairwise equal (rather than pairwise close), but without imposing any relation between the two pairs. For example, one admits trajectories $\alpha_1 = \alpha_2$ and $\alpha_3 = \alpha_4$ where α_2 and α_3 exit with the same transverse momentum p_{\perp} but at a classically different spatial coordinate y. When summed over the full family of trajectories, such configurations appear with rapidly oscillating phases, and their net contribution vanishes. 9,16,41 These rapidly oscillating phases disappear only if all four trajectories pass through the contact at equal positions and angles (up to quantum uncertainties), as is the case for the configurations shown in Figs. 3a and b.

C. Calculation of Q_6

The generic configuration of classical trajectories that contributes to Q_6 is shown in Fig. 5. Instead of dealing

with trajectories with one small-angle encounter, one now has to consider configurations of trajectories with two small-angle encounters or of trajectories with a 'three-encounter'. 34,35,36 A three-encounter arises when two encounters overlap, so that all six trajectories are within a phase space distance c simultaneously. In order to avoid confusion, we refer to non-overlapping encounters of two pairs of trajectories as 'two-encounters' for the remainder of this section. We first consider the case that all encounters fully reside inside the quantum dot. The case that encounters touch the lead openings will be discussed afterwards.

Without encounters that touch the lead openings, one distinguishes two types of contributions to Q_6 : the contribution from the case in which the trajectories undergo two separate two-encounters, and the contribution from the case in which the six classical trajectories involved undergo a three-encounter. These are shown in Fig. 5a and 5b, respectively. The configuration shown in Fig. 5a shows only one configuration with two two-encounters. There are two more configurations, which are obtained by the cyclic permutations $(1,2,i,j) \rightarrow (3,4,k,l) \rightarrow (5,6,m,n)$.

Because the two two-encounters in Fig. 5a do not overlap, their contribution $Q_6^{(5a)}$ to Q_6 factorizes. The stretch connecting the trajectories α_1 and α_2 to their joint entrance contact j contributes a factor $N_i/NF_2(1,2)$; the other stretches connecting the encounters to the contacts contribute similar factors to $Q_6^{(5a)}$. Further, using the results of the previous subsection, we find that the two-encounter of the trajectories α_1 , α_2 , α_3 , and α_4 in Fig. 5a contributes a factor $-F_4(1, 2, 3, 4) \exp(-\tau_{\rm E} F_4(1, 2, 3, 4)/\tau_{\rm D})$. Similarly, the two-encounter involving the trajectories α_1 , α_4 , α_5 , and α_6 contributes a factor $-F_4(1,4,5,6) \exp(-\tau_{\rm E}F_4(1,4,5,6)/\tau_{\rm D}).$ Finally, the stretch of the trajectories α_1 and α_4 that connects the two two-encounters in Fig. 5a contributes a factor $1/F_2(1,4)$. Using that $F_4(1,2,3,4) + F_4(1,4,5,6) = F_6(1,2,3,4,5,6) + F_2(1,4)$, we find that $Q_6^{(5a)}$ is given

$$Q_6^{(5a)} = \frac{N_i N_j N_k N_l N_m N_n e^{-\tau_{\rm E} F_6(1,2,3,4,5,6)/\tau_{\rm D}}}{N^6 F_2(1,2) F_2(3,2) F_2(3,4) F_2(5,4) F_2(5,6) F_2(1,6)} \left[\frac{F_4(1,2,3,4) F_4(1,4,5,6)}{F_2(1,4)} e^{-\tau_{\rm E} F_4(1,4)/\tau_{\rm D}} + \ldots \right], (49)$$

where the dots ... represent two more terms obtained by the cyclic permutations $(1, 2, i, j) \rightarrow (3, 4, k, l) \rightarrow (5, 6, m, n)$. As before, the superscript (5a) refers to the figure that shows the corresponding configuration of classical trajectories. Although the calculation of $Q_6^{(5b)}$ is similar in spirit, it proves rather cumbersome. Referring to App. B for details,

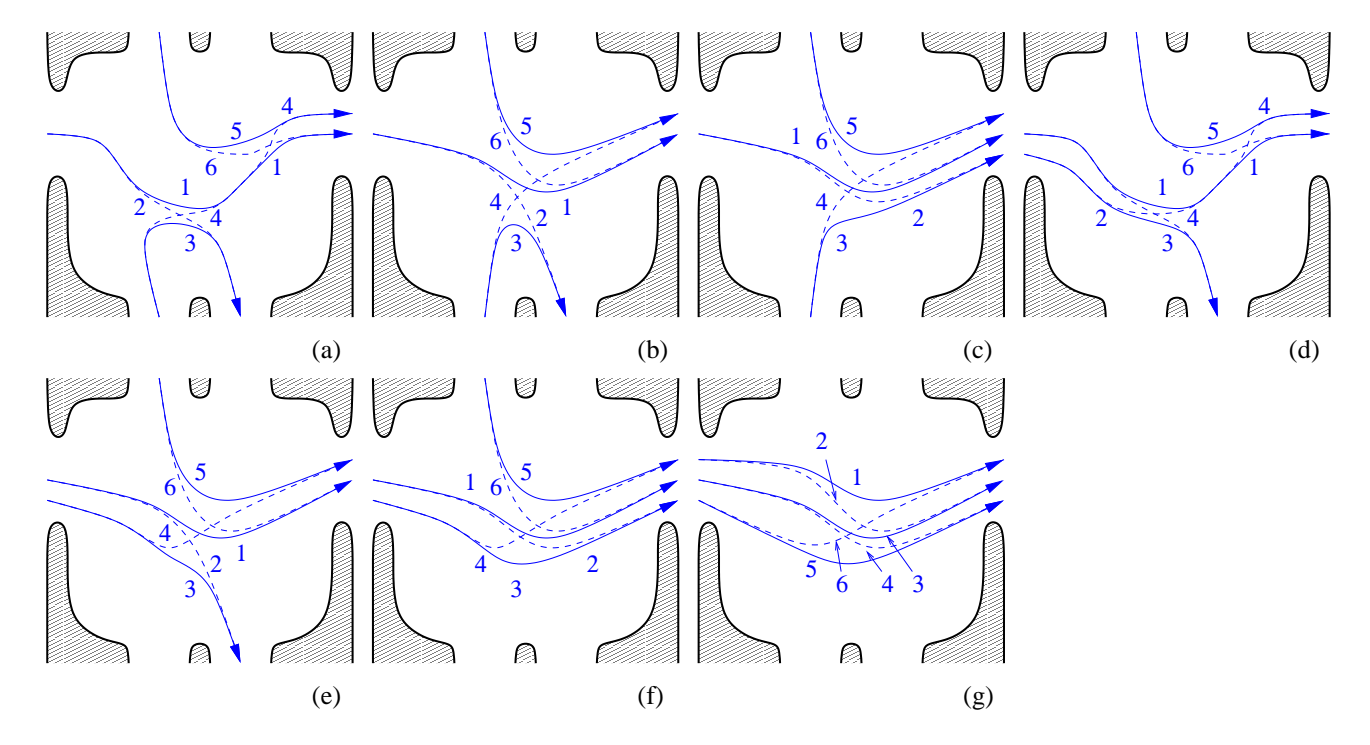


FIG. 6: Schematic drawing of six classical trajectories that provide the remaining contributions to Q_6 . The configuration shown in (a) consists of two separate two-encounters, where one two-encounter touches a lead opening. The configuration shown in (b) consists of one three-encounter, which partially touches one lead opening. The configuration of (c) consists of a three-encounter that fully touches one of the lead openings. The configuration of (d) has two two-encounters that each touch lead openings. The configuration of (e) has a three-encounter that partially touches two lead openings. The configuration of (f) has a three-encounter that partially touches one, and fully touches the other lead opening. Finally, the configuration of (g) fully touches both lead openings. The contributions from (a) and (b) have one Kronecker delta involving the lead indices, the contributions from (c), (d), and (e) have two Kronecker deltas, the contribution of (f) is zero, and the contribution of (g) has four Kronecker deltas.

we find

$$Q_{6}^{(5b)} = \frac{N_{i}N_{j}N_{k}N_{l}N_{m}N_{n}e^{-\tau_{E}F_{6}(1,2,3,4,5,6)/\tau_{D}}}{N^{6}F_{2}(1,2)F_{2}(3,2)F_{2}(3,4)F_{2}(5,4)F_{2}(5,6)F_{2}(1,6)} \left\{ \frac{F_{4}(1,2,3,4)F_{4}(1,4,5,6)}{F_{2}(1,4)} \left[1 - e^{-\tau_{E}F_{2}(1,4)/\tau_{D}} \right] + \dots \right\} - \frac{N_{i}N_{j}N_{k}N_{l}N_{m}N_{n}e^{-\tau_{E}F_{6}(1,2,3,4,5,6)/\tau_{D}}}{N^{6}F_{2}(1,2)F_{2}(3,2)F_{2}(3,4)F_{2}(5,4)F_{2}(5,6)F_{2}(1,6)} F_{6}(1,2,3,4,5,6).$$

$$(50)$$

Combining these two contributions, we find that the terms proportional to $\exp(-2\tau_{\rm E}/\tau_{\rm D})$ cancel, so that the final result is uniformly proportional to $\exp(-\tau_{\rm E}/\tau_{\rm D})$,

$$Q_{6}^{(5)} = \frac{N_{i}N_{j}N_{k}N_{l}N_{m}N_{n}e^{-\tau_{E}F_{6}(1,2,3,4,5,6)/\tau_{D}}}{N^{6}F_{2}(1,2)F_{2}(3,4)F_{2}(5,6)F_{2}(1,6)F_{2}(3,2)F_{2}(5,4)} \times \left[\frac{F_{4}(1,2,3,4)F_{4}(1,6,5,4)}{F_{2}(1,4)} + \frac{F_{4}(3,4,5,6)F_{4}(3,2,1,6)}{F_{2}(3,6)} + \frac{F_{4}(5,6,1,2)F_{4}(5,4,3,2)}{F_{2}(5,2)} + F_{6}(1,2,3,4,5,6)\right]. \tag{51}$$

In order to compute the contribution to Q_6 of encounters that touch the lead openings, we have to consider the configurations of classical trajectories shown in Fig. 6. Figure 6a show trajectories with two two-encounters where one encounter touches the lead opening. Figure 6b shows a configuration of classical trajectories with a three-encounter where the three-encounter partially touches a lead opening. In both cases, the escape of only one pair of trajectories is correlated, so that the contribution of the configurations of Figs. 6a and b has one Kronecker delta. In addition to the configurations shown in Fig. 6a and b, there five more contributions to Q_6 that are obtained by cyclic permutations of the trajectory labels and by the exchange of entrance and exit contacts. As before, the contribution from the

configuration with two two-encounters factorizes,

$$Q_{6}^{(6a)} = -\frac{N_{j}N_{l}N_{n}e^{-\tau_{E}F_{6}(1,2,3,4,5,6)/\tau_{D}}}{N^{3}F_{2}(1,2)F_{2}(3,4)F_{2}(5,6)} \left[\frac{N_{i}N_{k}F_{4}(1,2,3,4)\delta_{im}}{N^{2}F_{2}(2,3)F_{2}(1,4)} e^{-\tau_{E}F_{2}(1,4)/\tau_{D}} + \dots \right] - \frac{N_{i}N_{k}N_{m}e^{-\tau_{E}F_{6}(1,2,3,4,5,6)/\tau_{D}}}{N^{3}F_{2}(3,2)F_{2}(5,4)F_{2}(1,6)} \left[\frac{N_{j}N_{l}F_{4}(3,4,5,2)\delta_{jn}}{N^{2}F_{2}(3,4)F_{2}(5,2)} e^{-\tau_{E}F_{2}(5,2)/\tau_{D}} + \dots \right],$$
(52)

Details of the calculation of the three-encounter are again left to the appendix. The result is

$$Q_{6}^{(6b)} = -\frac{N_{j}N_{l}N_{n}e^{-\tau_{\rm E}F_{6}(1,2,3,4,5,6)/\tau_{\rm D}}}{N^{3}F_{2}(1,2)F_{2}(3,4)F_{2}(5,6)} \left[\frac{N_{i}N_{k}F_{4}(1,2,3,4)\delta_{im}}{N^{2}F_{2}(2,3)F_{2}(1,4)} \left(1 - e^{-\tau_{\rm E}F_{2}(1,4)/\tau_{\rm D}} \right) + \dots \right] - \frac{N_{i}N_{k}N_{m}e^{-\tau_{\rm E}F_{6}(1,2,3,4,5,6)/\tau_{\rm D}}}{N^{3}F_{2}(3,2)F_{2}(5,4)F_{2}(1,6)} \left[\frac{N_{j}N_{l}F_{4}(3,4,5,2)\delta_{jn}}{N^{2}F_{2}(3,4)F_{2}(5,2)} \left(1 - e^{-\tau_{\rm E}F_{2}(5,2)/\tau_{\rm D}} \right) + \dots \right].$$
 (53)

Combining both contributions, we again find that the terms proportional to $\exp(-2\tau_{\rm E}/\tau_{\rm D})$ cancel, so that

$$Q_6^{(6ab)} = \left[\frac{N_i N_j N_k N_l N_n \delta_{im} F_4(1, 2, 3, 4)}{N^5 F_2(1, 2) F_2(3, 2) F_2(3, 4) F_2(5, 6) F_2(1, 4)} + \frac{N_i N_j N_k N_l N_m \delta_{jn} F_4(3, 4, 5, 2)}{N^5 F_2(3, 2) F_2(3, 4) F_2(5, 4) F_2(1, 6) F_2(5, 2)} + \dots \right] \times e^{-\tau_{\rm E} F_6(1, 2, 3, 4, 5, 6) / \tau_{\rm D}}.$$
(54)

There are two different types of contributions to Q_6 with two Kronecker deltas: Two Kronecker deltas that both involve lead indices of entrance (or exit) leads, or a product of two Kronecker deltas, where one involves lead indices of the entrance lead and one involves lead indices of the exit lead. Only a configuration of trajectories with a three-encounter contribute to the former, see Fig. 6c, whereas configurations of trajectories with a three-encounter as well as configurations of trajectories with two two-encounters contribute to the latter, see Fig. 6d and e. Referring to the appendix for calculational details regarding the configurations of trajectories with a three-encounter, here we simply quote the results,

$$Q_{6}^{(6c)} = \left[\frac{N_{i}N_{j}N_{l}N_{n}\delta_{ik}\delta_{im}}{N^{4}F_{2}(1,2)F_{2}(3,4)F_{2}(5,6)} + \frac{N_{i}N_{j}N_{k}N_{m}\delta_{jl}\delta_{jn}}{N^{4}F_{2}(3,2)F_{2}(5,4)F_{2}(1,6)} \right] e^{-\tau_{\rm E}F_{6}(1,2,3,4,5,6)/\tau_{\rm D}},$$

$$Q_{6}^{(6de)} = \left[\frac{N_{i}N_{j}N_{l}N_{m}\delta_{ik}\delta_{ln}}{N^{4}F_{2}(1,2)F_{2}(3,6)F_{2}(5,4)} + \frac{N_{i}N_{j}N_{k}N_{n}\delta_{im}\delta_{jl}}{N^{4}F_{2}(1,4)F_{2}(3,2)F_{2}(5,6)} + \frac{N_{i}N_{j}N_{k}N_{l}\delta_{jn}\delta_{km}}{N^{4}F_{2}(1,6)F_{2}(3,4)F_{2}(5,2)} \right]$$

$$\times e^{-\tau_{\rm E}F_{6}(1,2,3,4,5,6)/\tau_{\rm D}}.$$

$$(56)$$

Finally, we have to consider the case that there is correlated escape of one pair and one triplet of trajectories and correlated escape of two triplets of trajectories, see Figs. 6f and g, respectively. One verifies that there is no contribution to Q_6 for the configuration shown in Fig. 6f. For the configuration shown in Fig. 6g one finds

$$Q_6^{(6g)} = \frac{N_i N_j \delta_{ik} \delta_{im} \delta_{jl} \delta_{jn}}{N^2 F_6(1, 2, 3, 4, 5, 6)} (1 - e^{-\tau_{\rm E} F_6(1, 2, 3, 4, 5, 6)/\tau_{\rm D}}).$$
(57)

Together, Eqs. (51), (54), (55), (56), and (57) combine to the effective random matrix theory ansatz for Q_6 .

IV. CONCLUSION

In this article we calculated the Ehrenfest-time dependence of the ensemble averages of polynomial functions Q_n of the $N \times N$ scattering matrix S of a ballistic chaotic

quantum dot and its hermitian conjugate S^{\dagger} , for polynomials of degree $n=2,\ 4,\ {\rm and}\ 6$. For all cases our calculations of the leading-in-N averages agreed with the effective random matrix theory of Silvestrov, Goorden, and Beenakker. ¹²

The detailed semiclassical calculations of Q_2 and Q_4 were included in this article because they are a prerequisite for the semiclassical calculations of Q_6 . For the calculation of Q_4 a few guiding principles would have been sufficient, however. These are: (i) the classical trajectories contributing to Q_4 have at most one small-angle encounter, (ii) each encounter lasts one Ehrenfest time $\tau_{\rm E}$, and (iii) Q_4 becomes equal to the classical limit $Q_4^{\rm cl}$ if $\tau_{\rm E}$ is much larger than the mean dwell time $\tau_{\rm D}$, whereas Q_4 equals the random matrix limit $Q_4^{\rm RMT}$ if $\tau_{\rm E} \ll \tau_{\rm D}$. From the first two guiding principles, both of which are well established in the literature, 1,6 and the exponential distribution of classical dwell times, one concludes that Q_4 is of the form

$$Q_4 = A + B \exp(-\tau_{\rm E}/\tau_{\rm D}). \tag{58}$$

The third guiding principle then fully determines the coefficients A and B and, hence, Q_4 .

No such shortcut exists for the calculation of Q_6 . The relevant configurations of semiclassical trajectories have up to two encounters, hence we expect a general form

$$Q_6 = A + B \exp(-\tau_E/\tau_D) + C \exp(-2\tau_E/\tau_D).$$
 (59)

The detailed calculation of this article was needed to show that the coefficient C=0. In this sense, the semiclassical calculation of Q_6 provides the first nontrivial test of the effective random matrix theory.

The fact that the coefficient C in Eq. (59) is zero is at the heart of the effective random matrix theory ansatz: It implies that (i) all trajectories with dwell times longer than $\tau_{\rm E}$ are treated equally and (ii) that $\tau_{\rm E}$ is the only time marking the boundary between classical and quantum effects. Whereas our calculation indirectly verifies these claims for leading-in-N averages of low-degree polynomials of S and S^{\dagger} , they are not true for subleadingin-N averages. For subleading-in-N averages, more than one integer multiple of $\tau_{\rm E}$ may determine quantum effects. Known examples are weak localization, to which only trajectories with a dwell time larger than $2\tau_{\rm E}$ contribute, although the weak localization correction is suppressed $\propto \exp(-\tau_{\rm E}/\tau_{\rm D})$ with an exponent containing $\tau_{\rm E}$, not $2\tau_{\rm E}$, 1,15,37 the leading quantum correction to the spectral form factor $K(\omega)$ of a quantum dot with broken time-reversal symmetry, 21 which has oscillations proportional to $\exp(2i\omega\tau_{\rm E})$, $\exp(3i\omega\tau_{\rm E})$, and $\exp(4i\omega\tau_{\rm E})$, conductance fluctuations in a bulk chaotic conductor (rather than a chaotic quantum dot), 42 and the mean square current pumped through a chaotic quantum dot with timedependent potentials.⁴³

Having verified the effective random matrix theory ansatz for leading-in-N averages for polynomials in S and S^{\dagger} up to degree six, one wonders whether this verification can be extended to polynomials of arbitrary degree. In our calculation, the simple result predicted by the effective random matrix theory was obtained only after a tedious calculation showing that the coefficient C in Eq. (59) above is zero. The possibility of the appearance of a term $\propto \exp(-2\tau_{\rm E}/\tau_{\rm D})$ caused a large increase in complexity upon going from polynomials of degree four to polynomials of degree six. We have searched for a simplification in our calculation that would allow us to cancel all contributions $\propto \exp(-2\tau_{\rm E}/\tau_{\rm D})$ at an earlier point in the calculation. However, since the terms proportional to $\exp(-2\tau_{\rm E}/\tau_{\rm D})$ were obtained from qualitatively different configurations of classical trajectories, we have not been able to find such a simplification. Without such a simplification, the task of extending the present calculation to polynomials of arbitrary degree seems too daunting to accomplish.

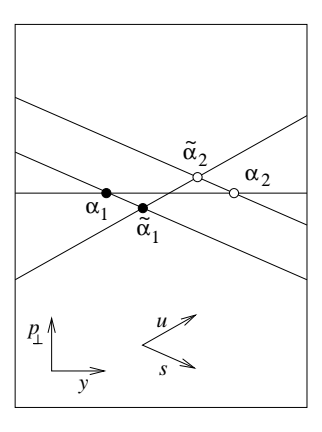


FIG. 7: Poincaré surface of section of lead opening, together with the standard coordinates y, p_{\perp} , as well as the phase space coordinates s, u, taken along the stable and unstable directions in phase space. The trajectory pair α_1, α_2 , which have equal perpendicular momentum components $p_{\perp,1} = p_{\perp,2}$ are mapped to a trajectory pair $\tilde{\alpha}_1, \tilde{\alpha}_2$ with equal stable phase space coordinates, $\tilde{s}_1 = \tilde{s}_2$. The unstable phase space coordinates do not change in the mapping.

Acknowledgments

We thank Maxim Vavilov for discussions. This work was supported by the NSF under grant no. DMR 0334499 and by the Packard Foundation.

APPENDIX A: TRAJECTORY SUM WITH FIXED COORDINATES s AND u'

In this appendix we show that one can replace the standard formulation in which the traces Q_n are expressed in terms of integrals over classical trajectories with specified transverse momentum components at entrance and exit contacts by an integral over classical trajectories with specified stable and unstable phase space coordinates at entrance and exit contacts, respectively.

We first consider a single integral over the transverse momentum p_{\perp} in the entrance contact,

$$K(p'_{\perp,1}, p'_{\perp,2}) = \frac{1}{2\pi\hbar} \int dp_{\perp} \sum_{\alpha_1, \alpha_2} A_1 A_2 e^{i(S_1 - S_2)/\hbar},$$
(A1)

where the trajectory α_{μ} has transverse momentum p_{\perp} at its entrance contact,

$$p_{\perp,1} = p_{\perp,2} = p_{\perp},$$
 (A2)

and transverse momentum $p'_{\perp,\mu}$ at its exit contact, $\mu = 1, 2$. The stability amplitude is given by Eq. (13). The classical action S_{μ} is a function of p_{\perp} and p'_{\perp} , $\mu = 1, 2$.

In order to rewrite K in terms of an integral over classical trajectories with a fixed stable phase space coordinate s upon entrance into the quantum dot, we consider a Poincaré surface of section taken at the entrance contact, see Fig. 7. There are two sets of coordinates to label

trajectories piercing this Poincaré surface of section: the spatial and momentum coordinates y and p_{\perp} , and the stable and unstable phase space coordinates s and u, see Fig. 7. The coordinate axes for s and u do not need to be perpendicular, but the coordinates are normalized such that $dsdu = dydp_{\perp}$. The phase space points where α_1 and α_2 pierce the Poincaré surface of section are indicated in the figure.

To each pair of two sufficiently close classical trajectories α_1 , α_2 we now assign another pair $\tilde{\alpha}_1$, $\tilde{\alpha}_2$, where the trajectory $\tilde{\alpha}_{\mu}$ is obtained from α_{μ} by slightly changing the boundary condition in the entrance contact while keeping the boundary condition upon exit the same. This implies that the unstable phase space coordinates of α_{μ} and $\tilde{\alpha}_{\mu}$ are equal, $\mu=1,2$. In order to uniquely define the pair $\tilde{\alpha}_1,\tilde{\alpha}_2$, we require that $\tilde{\alpha}_1$ and $\tilde{\alpha}_2$ have the same stable phase space coordinate s upon entry, and that $p_{\perp,\tilde{1}}-p_{\perp,1}=p_{\perp,2}-p_{\perp,\tilde{2}}$. The construction of $\tilde{\alpha}_1$ and $\tilde{\alpha}_2$ is shown in Fig. 7.

For this construction, one verifies that the action difference of the original and primed trajectory pair is not changed,

$$S_1 - S_2 = \tilde{S}_{\tilde{1}} - \tilde{S}_{\tilde{2}},\tag{A3}$$

provided we replace the action S, which is a function of p_{\perp} , by the action \tilde{S} , which is a function of the stable phase space coordinate s, obtained by Legendre transform of the original action S. Also, using the normalization $dsdu = dp_{\perp}dy$ and Eq. (A2), one finds

$$\int dp_{\perp} \left| \frac{\partial p'_{\perp,1}}{\partial y_1} \right|^{-1/2} \left| \frac{\partial p'_{\perp,2}}{\partial y_2} \right|^{-1/2} \dots =$$

$$\int ds \left| \frac{\partial p'_{\perp,\tilde{1}}}{\partial u_{\tilde{1}}} \right|^{-1/2} \left| \frac{\partial p'_{\perp,\tilde{2}}}{\partial u_{\tilde{2}}} \right|^{-1/2} \dots, \quad (A4)$$

where

$$s = s_{\tilde{1}} = s_{\tilde{2}}.\tag{A5}$$

The same procedure can be applied to integrations over the transverse momentum p'_{\perp} in the exit contacts. In this case, one replaces the integral over p'_{\perp} by an integral over the unstable phase space coordinate u', and replaces pairs of trajectories with equal p'_{\perp} by pairs of trajectories with equal u'. The result of this program is precisely Eqs. (19)–(21) of the main text.

APPENDIX B: THREE-ENCOUNTER OF CLASSICAL TRAJECTORIES

1. Three-encounter fully inside the quantum dot

In this appendix we describe the details of the calculation of $Q_6^{(5b)}$. This is the contribution to Q_6 from

a three-encounter that fully resides inside the quantum dot.

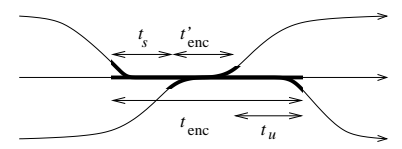


FIG. 8: Definition of the four measures of the encounter duration used in the text: $t_{\rm enc}$ is the total duration of the three-encounter, $t'_{\rm enc}$ is the duration of the part of the encounter that all trajectories involved in the three-encounter are within a phase-space distance c, and t_s and t_u are the durations of the encounter stretches where one pair of trajectories has already diverged from the remaining two pairs.

In order to calculate $Q_6^{(5b)}$, we take a Poincaré surface of section at a point that all six trajectories are within a phase space distance c. We parameterize the trajectories using phase space coordinates s and u along the stable and unstable directions in phase space. At the Poincaré surface of section, one has

$$s_1 = s_2, \quad s_3 = s_4, \quad s_5 = s_6$$

 $u_2 = u_3, \quad u_4 = u_5, \quad u_6 = u_1.$ (B1)

(These equalities continue to hold if the three-encounter touches the lead opening.) The action difference ΔS reads^{35,36}

$$\Delta S = (u_3 - u_1)(s_3 - s_1) + (u_5 - u_1)(s_5 - s_3) + \varepsilon_1 t_1 - \varepsilon_2 t_2 + \dots - \varepsilon_6 t_6.$$
 (B2)

In order to parameterize the durations of the six trajectories involved, we separate each duration t_{μ} , $\mu = 1, 2, ..., 6$, into segments before and after the encounter and one segment of duration $t_{\mu,\text{enc}}$ inside the encounter region. Similarly, we define

$$\Delta S_{\text{enc}} = (u_3 - u_1)(s_3 - s_1) + (u_5 - u_1)(s_5 - s_3) + \varepsilon_1 t_{1 \text{ enc}} - \varepsilon_2 t_{2 \text{ enc}} + \dots - \varepsilon_6 t_{6 \text{ enc}}.$$
(B3)

Integrating over the time segments outside the encounter, we then arrive at

$$Q_6^{(5b)} = \frac{N_i N_j N_k N_l N_m N_n}{N^6 F_2(1, 2) F_2(3, 4) F_2(5, 6) F_2(1, 6) F_2(3, 2) F_2(5, 4)} I,$$
(B4)

with

$$I = \tau_{\rm D} \int \frac{d(s_3 - s_1)d(s_5 - s_1)d(u_3 - u_1)d(u_5 - u_1)}{(2\pi\hbar)^2 t'_{\rm enc}} e^{i\Delta S_{\rm enc}/\hbar - t_{\rm enc}/\tau_{\rm D}}.$$
 (B5)

Here t_{enc} is the total duration of the encounter (the time that at least two trajectories are close together),

$$t_{\text{enc}} = \frac{1}{\lambda} \ln \frac{c}{\min(|s_3 - s_1|, |s_5 - s_1|, |s_3 - s_5|)} + \frac{1}{\lambda} \ln \frac{c}{\min(|u_3 - u_1|, |u_5 - u_1|, |u_3 - u_5|)},$$
(B6)

and t'_{enc} is the time that all three trajectories are close together, see Fig. 8,

$$t'_{\text{enc}} = \frac{1}{\lambda} \ln \frac{c}{\max(|s_3 - s_1|, |s_5 - s_1|, |s_3 - s_5|)} + \frac{1}{\lambda} \ln \frac{c}{\max(|u_3 - u_1|, |u_5 - u_1|, |u_3 - u_5|)}.$$
 (B7)

The factor t'_{enc} in the denominator cancels a spurious contribution to the integral arising from the freedom to choose the Poincaré surface of section at any point during three-encounter. The integration domain in Eq. (B5) is given by the conditions $\max(|u_3 - u_1|, |u_5 - u_1|, |u_3 - u_5|) < c$ and $\max(|s_3 - s_1|, |s_5 - s_1|, |s_3 - s_5|) < c$.

the conditions $\max(|u_3-u_1|, |u_5-u_1|, |u_3-u_5|) < c$ and $\max(|s_3-s_1|, |s_5-s_1|, |s_3-s_5|) < c$. We rewrite the integral (B5) using $s = \max(|s_3-s_1|, |s_5-s_1|, |s_3-s_5|)$, $s' = \min(|s_3-s_1|, |s_5-s_1|, |s_3-s_5|)$, $u = \max(|u_3-u_1|, |u_5-u_1|, |u_3-u_5|)$ and $u' = \min(|u_3-u_1|, |u_5-u_1|, |u_3-u_5|)$ as our integration variables. After some tedious algebra, one arrives at

$$I = \tau_{\rm D} \int_{0}^{c} ds du \int_{0}^{s/2} ds' \int_{0}^{u/2} du' \frac{e^{-t'_{\rm enc} F_{6}(1,2,3,4,5,6)/\tau_{\rm D}}}{(\pi \hbar)^{2} t'_{\rm enc}} \times \left\{ \left[e^{-F_{4}(1,2,5,6)t_{s}/\tau_{\rm D} - F_{4}(1,6,3,2)t_{u}/\tau_{\rm D}} + e^{-F_{4}(1,2,3,4)t_{s}/\tau_{\rm D} - F_{4}(1,6,3,2)t_{u}/\tau_{\rm D}} + \dots \right] \times \left(\cos \frac{us' + u's - us}{\hbar} + \cos \frac{us + u's' - u's}{\hbar} + \cos \frac{us + u's' - us'}{\hbar} + \cos \frac{us - u's'}{\hbar} \right) + 2 \left[e^{-F_{4}(1,2,3,4)t_{s}/\tau_{\rm D} - F_{4}(5,4,1,6)t_{u}/\tau_{\rm D}} + \dots \right] \left(\cos \frac{us' - u's' + su'}{\hbar} + \cos \frac{s'u - su'}{\hbar} \right) \right\},$$
(B8)

where the dots indicate cyclic permutations $(1,2) \rightarrow (3,4) \rightarrow (5,6)$, and with

We then perform the variable change

$$t'_{\text{enc}} = \frac{1}{\lambda} \ln \frac{c}{u} + \frac{1}{\lambda} \ln \frac{c}{s},$$

$$t_{s} = \frac{1}{\lambda} \ln \frac{s}{s'},$$

$$t_{u} = \frac{1}{\lambda} \ln \frac{u}{u'}.$$
(B9)

$$s = c/\sigma, \quad s' = cx'/\sigma,$$

 $u = cy\sigma, \quad u' = cyy'\sigma.$ (B10)

The total duration of the encounter is $t_{\text{enc}} = t'_{\text{enc}} + t_s + t_u$.

With these new variables, the integration over σ can be done and cancels the factor $t'_{\rm enc}$ in the denominator. Writing $r = c^2/\hbar$, the remaining integral then reads

$$I = \frac{\lambda \tau_{\rm D} r^2}{\pi^2} \int_0^{1/2} dx' dy' \int_0^1 y dy y^{F_6(1,2,3,4,5,6)/\lambda \tau_{\rm D}} \times \left\{ \left[(x')^{F_4(1,2,5,6)/\lambda \tau_{\rm D}} (y')^{F_4(1,6,3,2)/\lambda \tau_{\rm D}} + (x')^{F_4(1,2,3,4)/\lambda \tau_{\rm D}} (y')^{F_4(1,6,3,2)/\lambda \tau_{\rm D}} + \dots \right] \times \left[\cos(y r (x' + y' - 1)) + \cos(y r (1 + x'y' - y')) + \cos(y r (1 + x'y' - x')) + \cos(y r (1 - x'y')) \right] + 2 \left[(x')^{F_4(1,2,3,4)/\lambda \tau_{\rm D}} (y')^{F_4(5,4,1,6)/\lambda \tau_{\rm D}} + \dots \right] \left[\cos(y r (x' + y' - x'y') + \cos(y r (x' - y')) \right] \right\}.$$
 (B11)

In order to evaluate Eq. (B11), we write each product $(x')^{\epsilon_1}(y')^{\epsilon_2}$ as

$$(x')^{\epsilon_1}(y')^{\epsilon_2} = (1/2)^{\epsilon_1+\epsilon_2} + [(x')^{\epsilon_1} - (1/2)^{\epsilon_1}](1/2)^{\epsilon_2} + [(y')^{\epsilon_2} - (1/2)^{\epsilon_2}](1/2)^{\epsilon_1} + [(x')^{\epsilon_1} - (1/2)^{\epsilon_1}][(y')^{\epsilon_2} - (1/2)^{\epsilon_2}]$$
(B12)

and evaluate each of the four terms in Eq. (B12) separately. In Eq. (B12), the exponents ϵ_1 and ϵ_2 represent the exponents $F_4(1,2,5,6)/\lambda\tau_D$ etc. in Eq. (B11). The separation in Eq. (B12) makes sense, because both ϵ_1 and ϵ_2 are sent to zero if the classical limit $\hbar \to 0$ at fixed ratio τ_E/τ_D is taken. Hence, the first term in Eq. (B12) approaches unity, whereas the other terms are nonzero only if x' or y' are small, or both.

The four terms in Eq. (B12) are evaluated separately. For the first term in Eq. (B12), the integrals to x' and y' can be done exactly. Omitting a prefactor $(1/2)^{\epsilon_1+\epsilon_2}$, which is sent to 1 in the classical limit taken here, and abbreviating $\eta = F_6(1,2,3,4,5,6)/\lambda \tau_D$, we find that the integrals from the first term give

$$I_{1} = \frac{6\lambda\tau_{D}r^{2}}{\pi^{2}} \int_{0}^{1/2} dx'dy' \int_{0}^{1} dyyy^{\eta} [\cos(yr(x'+y'-1)) + \cos(yr(1+x'y'-y')) + \cos(yr(1+x'y'-x')) + \cos(yr(1-x'y')) + \cos(yr(x'+y'-x'y')) + \cos(yr(x'-y'))]$$

$$= \frac{6\lambda\tau_{D}}{\pi^{2}} \int_{0}^{1} dyy^{\eta} \frac{\partial}{\partial y} \left[-g_{c}(ry)\cos(ry) + g_{s}(ry)\sin(ry) \right],$$
(B13)

where

$$g_c(v) = \int_0^v dw \frac{1 - \cos w}{w}, \quad g_s(v) = \int_0^v dw \frac{\sin w}{w}.$$
 (B14)

Then, performing a partial integration to y and omitting terms that are oscillating with r, we find

$$I_{1} = \frac{6\lambda\tau_{D}\eta}{\pi^{2}} \int_{0}^{1} \frac{dy}{y} y^{\eta} \left[g_{c}(ry) \cos(ry) - g_{s}(ry) \sin(ry) \right], \tag{B15}$$

In this expression we can take the limits $r \to \infty$ and $\eta \to 0$, keeping $r^{-\eta} = e^{-\tau_{\rm E} F_6(1,2,3,4,5,6)/\tau_{\rm D}}$ fixed. We then find

$$I_1 = -F_6(1, 2, 3, 4, 5, 6)e^{-\tau_{\rm E}F_6(1, 2, 3, 4, 5, 6)/\tau_{\rm D}}.$$
 (B16)

For the second term in Eq. (B12), we first perform the integration to y', with the result

$$I_{2} = \frac{\lambda \tau_{D} r^{2}}{\pi^{2}} \int_{0}^{1/2} dx' dy' \int_{0}^{1} dyyy^{\eta} [(x')^{\epsilon} - (1/2)^{\epsilon}] [\cos(yr(x'+y'-1)) + \cos(yr(1+x'y'-y')) + \cos(yr(1+x'y'-x')) + \cos(yr(1-x'y')) + \cos(yr(x'+y'-x'y')) + \cos(yr(x'-y'))] + \dots$$

$$= \frac{\lambda \tau_{D}}{\pi^{2}} \int_{0}^{1/2} dx' \int_{0}^{1} dyy^{\eta} [(x')^{\epsilon} - (1/2)^{\epsilon}] \frac{\partial}{\partial y} \frac{x' \cos(yrx') - \cos(ry) + (1-x') \cos(yr(1-x'))}{x'(1-x')} + \dots, \quad (B17)$$

where we abbreviated $\epsilon = F_4(1,2,3,4)/\lambda \tau_D$. Performing a partial integration to y, omitting oscillating terms, we then find

$$I_{2} = \frac{\lambda \tau_{D}}{\pi^{2}} \int_{0}^{1/2} dx' (x'^{\epsilon} - (1/2)^{\epsilon}) \frac{\cos(rx')}{1 - x'} - \frac{F_{6}(1, 2, 3, 4, 5, 6)}{\pi^{2}} \int_{0}^{1/2} dx' (x'^{\epsilon} - (1/2)^{\epsilon}) \int_{0}^{1} \frac{dy}{y} y^{\eta} \frac{x' \cos(ryx') - \cos(ry) + (1 - x') \cos(yr(1 - x'))}{x'(1 - x')} + \dots$$
(B18)

The integral in the first line is of order 1/r and can be neglected in the limit $r \to \infty$. The integral in the second line is of order $\epsilon \propto 1/\lambda \tau_{\rm D}$, so that it can also be neglected. This is best seen by evaluating the integral after expanding $(x')^{\epsilon} - (1/2)^{\epsilon} \approx \epsilon \ln(2x')$ and replacing y^{η} by 1, which gives a finite value of the integral. Hence, we conclude that, in the classical limit $r \to \infty$ at fixed $r^{-1/\lambda \tau_{\rm D}}$, we have

$$I_2 = 0. (B19)$$

Similarly, one finds that the third term in Eq. (B12) does not contribute to I.

For the remaining contribution I_4 , we note that the only nonzero contribution can come from small x' and small y'. Neglecting x' and y' with respect to unity, one finds that the contribution from the first term between brackets $\{\ldots\}$ in Eq. (B11) gives zero. In the same approximation, after two partial integrations the second term gives

$$I_4 = \frac{4\lambda \tau_{\rm D} \epsilon_1 \epsilon_2}{\pi^2} \int_0^{1/2} \frac{dx' dy'}{x'y'} \int_0^1 dy y^{\eta - 1} (x')^{\epsilon_1} (y')^{\epsilon_2} \sin(yrx') \sin(yry') + \dots,$$
(B20)

where $\epsilon_1 = F_4(1, 2, 3, 4)/\lambda \tau_D$ and $\epsilon_2 = F_4(5, 4, 1, 6)$ (or cyclic permutations), and $\eta = F_6(1, 2, 3, 4, 5, 6)/\lambda \tau_D$. We then shift variables x' = x''/y and y' = y''/y and integrate over y,

$$I_{4} = \frac{4\lambda\tau_{D}\epsilon_{1}\epsilon_{2}}{\pi^{2}(\epsilon_{1}+\epsilon_{2}-\eta)} \int_{0}^{1/2} \frac{dx''dy''}{x''y''} (x'')^{\epsilon_{1}} (y'')^{\epsilon_{1}} [(\max(x'',y''))^{\eta-\epsilon_{1}-\epsilon_{2}} - (1/2)^{\eta-\epsilon_{1}-\epsilon_{2}}] \sin(rx'') \sin(ry'') + \dots$$

$$= \frac{F_{4}(1,2,3,4)F_{2}(5,4,1,6)}{F_{2}(1,4)} e^{-\tau_{E}F_{6}(1,2,3,4,5,6)/\tau_{D}} \left[1 - e^{-\tau_{E}F_{2}(1,4)/\tau_{D}}\right] + \dots, \tag{B21}$$

where we used that $F_4(1,2,3,4) + F_4(5,4,1,6) - F_6(1,2,3,4,5,6) = F_2(1,4)$. As before, the dots ... refer to the two additional terms obtained by cyclic permutation $(1,2) \to (3,4) \to (5,6)$ of the expression written above.

The final result for $Q_6^{(5b)}$ is found by substituting $I = I_1 + I_4$ into Eq. (B4).

2. Three-encounter that touches the lead openings

If the three-encounter touches the lead openings, escape of the trajectories involved in the encounter is no longer uncorrelated. In order to deal with threeencounters that touch the lead openings, the initial part of the calculation of the previous subsection has to be modified. However, the final integrals will all be of the form of the integrals I_1 , I_2 , and I_4 calculated above. Here we discuss the configurations of Figs. 6b and c in detail. The calculation of the remaining configurations (Figs. 6eg) proceeds in a similar manner. In the discussion here we further limit ourselves to the labeling of trajectories as shown in the figure. For Fig. 6b, this means that we consider the exit of trajectories α_1 and α_5 to be correlated, whereas the exit of trajectory α_3 , as well as all entrances are uncorrelated. There are five more contributions to Q_6 : two of these arise from configurations where the exit of α_1 and α_3 or the exit of α_3 and α_5 is correlated; three more arise from configurations with correlated entry of two trajectories, and uncorrelated exits. For Fig. 6c, we take the exits of all trajectories to be correlated, whereas the entrances are not. There is another contribution obtained by reversing the roles of entrance and exit.

In order to describe a three-encounter that touches the lead opening as shown in Fig. 6b, we again take a Poincaré surface of section at a point that all six trajectories are within a phase space distance c. In the configuration of Fig. 6b, this 'central' part of the three-encounter does not touch a lead opening. We ensure that α_3 has moved away from the other trajectories before arriving

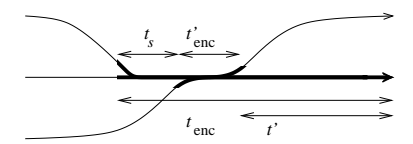


FIG. 9: Definition of the four measures of the encounter duration used in the text: $t_{\rm enc}$ is the total duration of the three-encounter, $t'_{\rm enc}$ is the duration of the part of the encounter that all trajectories involved in the three-encounter are within a phase-space distance c, and t_s and t' are the durations of the encounter stretches where one pair of trajectories has already diverged from the remaining two pairs. The right end of the encounter is at the lead opening.

at the lead opening by requiring

$$\min(|u_1 - u_3|, |u_5 - u_3|) > |u_1 - u_5|.$$
 (B22)

The escape of α_1 and α_5 is correlated if

$$0 < t' < t_u, \tag{B23}$$

where

$$t_u = \frac{1}{\lambda} \ln \frac{\max(|u_3 - u_1|, |u_3 - u_5|)}{|u_5 - u_1|},$$
 (B24)

and t' is the duration of the stretch of the encounter immediately adjacent to the lead opening, during which α_1 and α_5 are correlated with each other, but not with α_3 , see Fig. 9. We then find

$$Q_6^{(6b)} = \frac{N_i N_j N_k N_l N_n \delta_{im}}{N^5 F_2(1, 2) F_2(3, 4) F_2(5, 6) F_2(3, 2)} I, \text{ (B25)}$$

where

$$I = \int d(s_3 - s_1) d(s_5 - s_1) d(u_3 - u_1) d(u_5 - u_1)$$

$$\times \int \frac{dt'}{\tau_{\rm D}} \frac{e^{i\Delta S_{\rm enc} - t_{\rm enc}/\tau_{\rm D}}}{(2\pi\hbar)^2 t'_{\rm enc}}, \tag{B26}$$

with

The action difference $\Delta S_{\rm enc}$ is given by Eq. (B3) above.

$$t_{\text{enc}} = t' + t'_{\text{enc}} + t_s,$$

$$t'_{\text{enc}} = \frac{1}{\lambda} \ln \frac{c}{\max(|u_3 - u_1|, |u_3 - u_5|)}$$

$$+ \frac{1}{\lambda} \ln \frac{c}{\max(|s_1 - s_3|, |s_1 - s_5|, |s_3 - s_5|)} .$$

$$t_s = \frac{1}{\lambda} \ln \frac{\max(|s_1 - s_3|, |s_1 - s_5|, |s_3 - s_5|)}{\min(|s_1 - s_3|, |s_1 - s_5|, |s_3 - s_5|)} .$$
 (B28)

Rewriting the integral in terms of the variables $s = \max(|s_1 - s_3|, |s_1 - s_5|, |s_3 - s_5|), s' = \min(|s_1 - s_3|, |s_1 - s_5|, |s_3 - s_5|), u = \max(|u_3 - u_1|, |u_3 - u_5|), \text{ and } u' = |u_5 - u_1|, \text{ and integrating over } t', \text{ we arrive at}$

$$I = \tau_{\rm D} \int_{0}^{c} ds \int_{0}^{s/2} ds' \int_{0}^{c} du \int_{0}^{u/2} du' \frac{e^{-t'_{\rm enc}F_{6}(1,2,3,4,5,6)/\tau_{\rm D}}}{(\pi\hbar)^{2}t'_{\rm enc}F_{4}(5,4,1,6)} \left[1 - e^{-t_{u}F_{4}(1,4,5,6)/\tau_{\rm D}}\right]$$

$$\times \left\{ \left(e^{-t_{s}F_{4}(1,2,5,6)/\tau_{\rm D}} + e^{-t_{s}F_{4}(3,4,5,6)/\tau_{\rm D}}\right) \right.$$

$$\times \left(\cos \frac{us + u's' - u's}{\hbar} + \cos \frac{us - us' - u's}{\hbar} + \cos \frac{us - u's'}{\hbar} + \cos \frac{us - us' + u's'}{\hbar}\right)$$

$$\left. + 2e^{-t_{s}F_{4}(1,2,3,4)/\tau_{\rm D}} \left(\cos \frac{us' - u's}{\hbar} + \cos \frac{us' + u's - us'}{\hbar}\right) \right\},$$
(B29)

We now change variables

$$s = c/\sigma, \quad s' = cx'/\sigma, \quad u = cy\sigma, \quad u' = cyy'\sigma.$$
 (B30)

Writing $r = c^2/\hbar$ and integrating over σ , the integral then reads

$$I = \frac{\lambda \tau_{\rm D} r^2}{\pi^2 F_4(5,4,1,6)} \int_0^{1/2} dx' \int_0^{1/2} dy' \int_0^1 y dy y^{F_6(1,2,3,4,5,6)/\lambda \tau_{\rm D}} [1 - (y')^{F_4(1,4,5,6)/\lambda \tau_{\rm D}}]$$

$$\times \left\{ [(x')^{F_4(1,2,5,6)/\lambda \tau_{\rm D}} + (x')^{F_4(3,4,5,6)/\lambda \tau_{\rm D}}] \right.$$

$$\times \left[\cos(yr(1+y'x'-y')) + \cos(yr(1-x'-y') + \cos(yr(1-x'y')) + \cos(yr(1-x'+y'x'))) \right]$$

$$\left. + 2(x')^{F_4(1,2,3,4)/\lambda \tau_{\rm D}} [\cos(yr(x'+y'-x'y')) + \cos(yr(x'-y'))] \right\}.$$
(B31)

The remainder of the calculation is identical to that of the previous subsection: We write

$$(x')^{\epsilon} = 1 + ((x')^{\epsilon} - (1/2)^{\epsilon}), \tag{B32}$$

where ϵ represents $F_4(1,2,5,6)/\lambda \tau_D$, $F_4(3,4,5,6)/\lambda \tau_D$, or $F_4(1,2,3,4)/\lambda \tau_D$, and evaluate the two terms in Eq. (B32) separately. The calculation of the first term is identical to that of I_2 , see Eqs. (B17)–(B19), and vanishes. The calculation of the second term is identical to that of I_4 , see Eq. (B21) above. We thus find

$$I = -\frac{F_4(1,2,3,4)}{F_2(1,4)}e^{-\tau_{\rm E}F_6(1,2,3,4,5,6)/\tau_{\rm D}} \left[1 - e^{-\tau_{\rm E}F_2(1,4)/\tau_{\rm D}}\right]. \tag{B33}$$

Substitution of Eq. (B33) into Eq. (B25) and addition of the remaining five configurations of trajectories obtained by relabeling or by interchanging entrance and exit gives Eq. (53).

Proceeding in a similar manner for the case shown in Fig. 6c, we find

$$Q_6^{6c} = \frac{N_i N_j N_l N_n \delta_{ik} \delta_{im}}{N^4 F_2(1, 2) F_2(3, 4) F_2(5, 6)} I, \quad (B34)$$

where

$$I = \tau_{\rm D} \int d(s_3 - s_1) d(s_5 - s_1) d(u_3 - u_1) d(u_5 - u_1) \times \int \frac{dt'_{\rm enc}}{\tau_{\rm D}} \frac{e^{i\Delta S_{\rm enc}/\hbar - t_{\rm enc}/\tau_{\rm D}}}{(2\pi\hbar)^2 t'_{\rm enc}},$$
(B35)

with

$$t_{\text{enc}} = t'_{\text{enc}} + \frac{1}{\lambda} \ln \frac{\max(|s_1 - s_3|, |s_1 - s_5|, |s_3 - s_5|)}{\min(|s_1 - s_3|, |s_1 - s_5|, |s_3 - s_5|)}.$$
(B36)

We require

$$0 < t'_{\text{enc}} < \frac{1}{\lambda} \ln \frac{c}{\max(|s_1 - s_3|, |s_1 - s_5|, |s_3 - s_5|)} + \frac{1}{\lambda} \ln \frac{c}{\max(|u_1 - u_3|, |u_1 - u_5|, |u_3 - u_5|)},$$
(B37)

in order to ensure that the three-encounter indeed touches the lead opening at a point that all trajectories involved in the encounter are separated by phase space distances less than the cut-off c. The integration over $t'_{\rm enc}$ can be done immediately. Rewriting the integral in terms of the variables $s = \max(|s_1 - s_3|, |s_1 - s_5|, |s_3 - s_5|), s' = \min(|s_1 - s_3|, |s_1 - s_5|, |s_3 - s_5|), u = \max(|u_1 - u_3|, |u_1 - u_5|, |u_3 - u_5|),$ and $u' = \min(|u_1 - u_3|, |u_1 - u_5|, |u_3 - u_5|),$ and performing the variable change

$$s = c/\sigma$$
, $s' = cx'/\sigma$, $u = cy\sigma$, $u' = cyy'\sigma$, (B38)

we arrive at the integral

$$I = \frac{2\lambda\tau_{\rm D}r^2}{\pi^2 F_6(1,2,3,4,5,6)} \int_0^{1/2} dx' dy' \int_0^1 y dy [1 - y^{F_6(1,2,3,4,5,6)/\lambda\tau_{\rm D}}] \left[(x')^{F_4(1,2,5,6)/\lambda\tau_{\rm D}} + \ldots \right] \times \left[\cos(yr(1+y'x'-y')) + \cos(yr(1-x'-y') + \cos(yr(1-x'y')) + \cos(yr(1-x'+y'x')) + \cos(yr(x'+y'-x'y')) + \cos(yr(x'-y')) \right]. \tag{B39}$$

In this integral, the contribution from the term 1 in $[1-y^{F_6(1,2,3,4,5,6)/\lambda\tau_{\rm D}}]$ vanishes. Writing $(x')^\epsilon=(1/2)^\epsilon+((x')^\epsilon-(1/2)^\epsilon)$, with $\epsilon=F_4(1,2,5,6)/\lambda\tau_{\rm D}$ etc., we arrive at integrals identical to the integrals I_1 and I_2 considered in the previous subsection. We thus find

$$I = e^{-\tau_{\rm E} F_6(1,2,3,4,5,6)/\tau_{\rm D}}.$$
 (B40)

Substituting this result into Eq. (B34) and adding what one obtains after interchanging entrance and exit leads, one arrives at Eq. (55).

The remaining configurations of trajectories with a three-encounter (Figs. 6e and 6) are treated in the same manner.

¹ I. L. Aleiner and A. I. Larkin, Phys. Rev. B **54**, 14423 (1996).

A. I. Larkin and Y. N. Ovchinnikov, Zh. Eksp. Teor. Fiz. 55, 2262 (1968) [Sov. Phys. JETP 28, 1200 (1969)].

³ G. M. Zaslavsky, Phys. Rep. **80**, 157 (1981).

⁴ L. P. Kouwenhoven, C. M. Marcus, P. L. McEuen, S. Tarucha, R. M. Westervelt, and N. S. Wingreen, in Mesoscopic Electron Transport, edited by L. L. Sohn, L. P. Kouwenhoven, and G. Schön (Kluwer, Dordrecht, 1997), vol. 345 of NATO ASI Series E.

⁵ C. W. J. Beenakker, Rev. Mod. Phys. **69**, 731 (1997).

⁶ O. Agam, I. Aleiner, and A. Larkin, Phys. Rev. Lett. 85, 3153 (2000).

⁷ P. G. Silvestrov, M. C. Goorden, and C. W. J. Beenakker, Phys. Rev. B **67**, 241301 (2003).

⁸ J. Tworzydlo, A. Tajic, H. Schomerus, and C. W. J. Beenakker, Phys. Rev. B 68, 115313 (2003).

⁹ R. S. Whitney and P. Jacquod, Phys. Rev. Lett. **94**, 116801 (2005).

¹⁰ I. Adagideli and C. W. J. Beenakker, Phys. Rev. Lett. 89, 237002 (2002).

¹¹ M. G. Vavilov and A. I. Larkin, Phys. Rev. B **67**, 115335 (2003).

¹² P. G. Silvestrov, M. C. Goorden, and C. W. J. Beenakker, Phys. Rev. Lett. **90**, 116801 (2003).

¹³ C. W. J. Beenakker, Lect. Notes Phys. **667**, 131 (2005), cond-mat/0406018.

¹⁴ I. Adagideli, Phys. Rev. B **68**, 233308 (2003).

¹⁵ S. Rahav and P. W. Brouwer, Phys. Rev. Lett. **95**, 056806 (2005).

¹⁶ P. Jacquod and R. S. Whitney, cond-mat/0512662 (2005).

¹⁷ J. Tworzydlo, A. Tajic, and C. W. J. Beenakker, Phys. Rev. B **69**, 165318 (2004).

¹⁸ P. Jacquod and E. V. Sukhorukov, Phys. Rev. Lett. **92**, 116801 (2004).

¹⁹ P. W. Brouwer and S. Rahav, cond-mat/0512095 (2005).

²⁰ I. L. Aleiner and A. I. Larkin, Phys. Rev. E **55**, 1243(R) (1997).

²¹ C. Tian and A. I. Larkin, Phys. Rev. B **70**, 035305 (2004).

²² J. Tworzydlo, A. Tajic, H. Schomerus, P. W. Brouwer, and C. W. J. Beenakker, Phys. Rev. Lett. **93**, 186806 (2004).

²³ M. C. Goorden, P. Jacquod, and C. W. J. Beenakker, Phys. Rev. B **72**, 064526 (2005).

²⁴ H. Schomerus and P. Jacquod, J. Phys. A **38**, 10663 (2005).

²⁵ H. Schomerus and J. Tworzydlo, Phys. Rev. Lett. **93**, 154102 (2004).

²⁶ Y. M. Blanter and M. Büttiker, Phys. Rep. **336**, 1 (2000).

²⁷ R. Blümel and U. Smilansky, Phys. Rev. Lett. **60**, 477 (1988).

²⁸ M. L. Polianski and P. W. Brouwer, J. Phys. A **36**, 3215

- (2003).
- ²⁹ P. W. Brouwer, A. Lamacraft, and K. Flensberg, Phys. Rev. B **72**, 075316 (2005).
- ³⁰ R. A. Jalabert, H. U. Baranger, and A. D. Stone, Phys. Rev. Lett. **65**, 2442 (1990).
- ³¹ H. U. Baranger, R. A. Jalabert, and A. D. Stone, Phys. Rev. Lett. **70**, 3876 (1993).
- ³² H. U. Baranger, R. A. Jalabert, and A. D. Stone, Chaos 3, 665 (1993).
- ³³ P. Braun, S. Heusler, S. Müller, and F. Haake, condmat/051192 (2005).
- ³⁴ S. Heusler, S. Müller, P. Braun, and F. Haake, Phys. Rev. Lett. **96**, 066804 (2006).
- ³⁵ S. Müller, S. Heusler, P. Braun, F. Haake, and A. Altland, Phys. Rev. Lett. **93**, 014103 (2004).
- ³⁶ S. Müller, S. Heusler, P. Braun, F. Haake, and A. Altland, Phys. Rev. E **72**, 046207 (2005).

- ³⁷ K. Richter and M. Sieber, Phys. Rev. Lett. **89**, 206801 (2002).
- ³⁸ D. Spehner, J. Phys. A **36**, 7269 (2003).
- ³⁹ M. Turek and K. Richter, J. Phys. A **36**, L455 (2003).
- ⁴⁰ Strictly speaking, one should also include trajectories for which transverse momenta components are opposite, cf. Eq (12). However in that case the summation over trajectories contains a rapidly oscillating phase, so that their net contribution to the sum vanishes in the classical limit, see, e.g., Refs. 9,16,41.
- 41 S. Rahav and P. W. Brouwer, Phys. Rev. Lett. 96, 196804 (2006).
- ⁴² C. Tian, A. Altland, and P. W. Brouwer, condmat/0605051 (2006).
- ⁴³ S. Rahav and P. W. Brouwer, unpublished (2006).